Turkish Journal of Electrical Engineering & Computer Sciences

http://journals.tubitak.gov.tr/elektrik/

Research Article

Turk J Elec Eng & Comp Sci
(2013) 21: 1842 – 1856

doi:10.3906/elk-1202-71

A combined protective scheme for fault classification and identification of faulty section in series compensated transmission lines

Resul ÇÖTELİ*
Department of Energy Systems Engineering, Faculty of Technology, Fırat University, Elazığ, Turkey

Received: 17.02.2012 • **Accepted:** 18.06.2012 • **Published Online:** 24.10.2013 • **Printed:** 18.11.2013

Abstract: The fault detection process is very difficult in transmission lines with a fixed series capacitor because of the nonlinear behavior of protection device and series-parallel resonance. This paper proposes a new method based on S-transform (ST) and support vector machines (SVMs) for fault classification and identification of a faulty section in a transmission line with a fixed series capacitor placed at the middle of the line. In the proposed method, the fault detection process is carried out by using distinctive features of 3-line signals (line voltages and currents) and zero sequence current. The relevant features of these signals are obtained by using the ST. The obtained features are then used as input to multiple SVM classifiers and their outputs are combined for classifying the fault type and identifying the faulty section. Training and testing samples for the proposed method have been generated with different types of short-circuit faults and different combinations of system parameters in the MATLAB environment. The performance of the proposed method is investigated according to the accuracy of fault classification and faulty section identification. To evaluate the validity of this study, the proposed method is also compared to both ST–neural network and previous studies. The proposed method not only provides a good classification performance for all types of faults, but also detects the faulty section at a high accuracy.

Key words: Fault classification, faulty section identification, series compensated transmission line, S-transform, support vector machines

1. Introduction

Today, series compensation is a necessity to improve the power transfer capacity of transmission lines. Unlike shunt compensation, the purpose of series compensation is to modify electrical characteristics of transmission lines. Consequently, power transfer capability of the line is increased, the voltage profile of the line is improved, and systems losses are reduced. In this type of compensation, the capacitor banks can be installed anywhere on the transmission line. Commonly, series compensation architecture consists of the capacitor banks and a protective system to prevent the capacitor against overvoltage, called a metal oxide varistor (MOV). The MOV includes a bypass gap, damping reactor, and bypass circuit breaker. The bypass gap is controlled to spark over in the event of excess varistor energy. The bypass breaker closes automatically in the case of prolonged gap conduction or other platform contingencies. The breaker also allows the operator to insert or bypass the series capacitor. The damping reactor limits the capacitor discharge resulting from gap spark over or bypassing the breaker closure [1].

Although series compensation systems offer many advantages to power system operations, the distance

*Correspondence: rcoteli@firat.edu.tr

protection task in the series compensated transmission lines (SCTLs) is more difficult than in uncompensated lines. This is because the nonlinear behavior of a series capacitor arrangement during fault conditions affects the current-voltage signals, and nonstationary and nonperiodic signals may appear in fault cases [2]. Therefore, classification and identification of faults for relaying decisions and autoclosing are difficult tasks in SCTLs [3].

The digital protective relays based on traditional signal processing methods such as full-cycle discrete Fourier transform, half-cycle discrete Fourier transform, and least square error may not provide a reliable protection for series compensated lines since they fail to process the signals accurately in the presence of nonstationary and nonperiodic signals. Moreover, phasor estimation requires a sliding window of a cycle that may cause a significant delay [4–7]. Therefore, such techniques may not give satisfactory results for fault detection in SCTLs [8].

To eliminate disadvantages of conventional techniques, different methods have been proposed for fault classification and faulty section identification in SCTLs. In [9] and [10–15], fuzzy logic and neural networks (NNs) were proposed for fault classification in SCTLs, respectively. In NNs and fuzzy logic-based approaches, there are many parameters to be adjusted. In addition, the learning of a NN has usually been performed by using gradient-based learning algorithms and such methods have several drawbacks, such as the difficulty in setting learning parameters, slow convergence, slow learning, and training failures [16]. Decision tree-based protection schemes were proposed in [17]. The support vector machine (SVM) method was applied for the identification of a faulty section in an advanced SCTL in [3] and [18]. In [19], multiclass SVM and an extreme learning machine were used for fault classification in SCTLs.

The wavelet transform (WT)-based relaying schemas have been also proposed for protection of SCTLs in the literature [20]. WTs have some drawbacks such as selection of the mother wavelet, sensitivity to noise, lack of absolute referenced phase information, production of unsuitable time-scale plots for intuitive visual analysis, and delay due to its batch processing [21–23]. In [2] and [8], combined techniques such as WT-fuzzy logic and WT-SVM were also proposed for protection of SCTLs, respectively.

The S-transform (ST), which is a superior method for time-frequency analysis, is a hybrid signal processing method combining the advantages of short-time Fourier transform and WT. The basic idea of the ST is to obtain a time-frequency energy distribution of the signal to isolate and process independently the components of the signal in the time-frequency plane. In the ST, a scalable and variable window length is used and a Fourier kernel is employed to provide the phase information referenced to the time origin. Hence, it provides supplementary information about spectra that is not available from the locally referenced phase obtained by the continuous WT [23].

Recently, the ST has been applied to power quality events in electric power systems [24,25]. Moreover, studies in the literature have shown that the ST is more robust to noise than the WT [24,25]. Therefore, a more reliable protection of SCTLs may be achieved by means of the ST. There are several publications using the ST in the literature to classify and identify faults in transmission lines [26–28]. In [26] and [27], ST and a probabilistic neural network, and ST and a logistic model tree (LMT), were proposed for a transmission line including FACTS devices (thyristor-controlled series compensator), respectively. In addition, the method proposed in [27] was evaluated over limited test cases such as 200 datasets and 6 features obtained from the ST were used for classification and section identification. In [28], a ST and NN for HVDC lines were also proposed. The main drawbacks of NNs are well known. Moreover, LMTs have the computational complexity of inducing the logistic regression models in a tree. Recently, SVMs have been used as an attractive tool for

pattern classification because of their superior features such as producing single, optimum, and automatic sparse solutions by simultaneously minimizing both generalization and training error and separating data by a large margin in high-dimensional space [29]. Furthermore, no study has been reported yet about ST-SVM–based protection schema for SCTLs with fixed capacitors.

This paper proposes a combined method based on the ST and SVM for automatic classification of faults and identification of faulty sections occurring in SCTLs with a fixed capacitor. In the proposed method, 3-line signals (voltage and current) and zero sequence current sensed from the sending end are used for fault classification and identification of the faulty sections. The distinctive features of the postfault voltages and currents are extracted by the ST approach. From each sensed signal, the 8 distinctive features covering maximum, minimum, standard deviation and magnitude factor of maximum amplitude-time plot (TMA-plot), total harmonic distortion and mean square root of frequency-maximum amplitude plot (FMA-plot), standard deviation of frequency-time (TF) contour, and energy of the largest frequency amplitude of TF-contour are extracted by using the ST. Features obtained from voltage and current signals are then entered into SVMs of respective phases. SVMs used for line current and voltage signals have 2 inputs and 2 outputs, and their outputs represent a faulty phase and faulty section. A SVM used for zero sequence current has 1 input and 1 output, and its output designates the ground fault. In order to evaluate the performance of the proposed technique, extensive simulation studies are performed by means of a model built in MATLAB. The simulation model consists of transmission line, 2 generators, and a series capacitor placed at the midpoint of line. A total of 30,240 training and test cases are generated with different combinations of fault types and system parameters. Performance of the proposed method is evaluated over an extensive set of 27,240 test cases, which are not introduced to the classifier in training stage. In addition, test cases are randomly selected from the dataset. The performance comparisons between the proposed method and combined ST-NN method as well as previous studies are given for a better validation.

2. Case studies

The validity of the proposed technique is evaluated by the simulation model constructed in MATLAB/Power System Toolbox. The schematic diagram of the simulated system is shown in Figure 1 and system parameters are given in Table 1. The model consists of 2 generators connected to a transmission line of 320 km with a series capacitor placed at the middle of the line. The transmission line is a distributed parameter line model with lumped losses. The overvoltage protection of the series capacitor is provided by a MOV and the air gap. A load with lagging factor is connected to the transmission line. A sampling frequency of 16 kHz is used in the simulation studies.

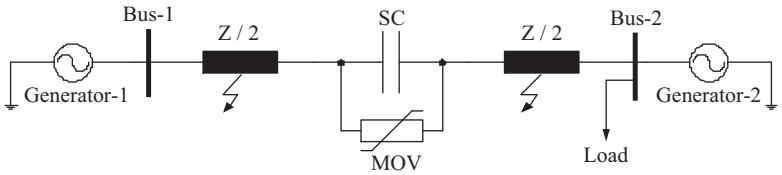

Figure 1. The schematic diagram of the simulated system.

Extensive simulation studies are carried out for different combinations of source impedances, fault resistances (FRs), load angles (LAs), fault inception angles (FIAs), faults in front of the series compensator (*fsc*) as well as behind (*bsc*), fault location, and percentage compensation levels (CLs). In addition, different

types of short-circuit faults including line-ground (LG), line-line (LL), line-line-ground (LLG), and 3-line/3-line-ground (LLL-LLLG) faults are considered for each of these combinations. An example presentation of LG faults including *fsc* is given in Table 2. This table can be expanded for other fault types and faulty sections. In the simulation studies, impedance of generator-1 is also changed to 75% and 100%, whereas impedance of generator-2 is kept constant at 100%.

Table 1. System parameters used in the simulation model.

Transmission line	Length (km)	320
	Voltage (kV)	400
	Positive sequence impedance (Ω)	4.0736 + j93.81
	Zero sequence impedance (Ω)	123.648 + j414.6
	Positive sequence capacitance (mF/km)	4.077
	Zero sequence capacitance (mF/km)	2.48
Generators	Impedance (Ω)	0.5333 + j5.333
	Frequency (Hz)	50
Load	Active power	400 MW
	Reactive power	330 MVar

Table 2. Studied LG faults for different combinations of system parameters.

FIA (°)	CL (%)	FR (Ω)	LA (°)	FL (km)
0–45–90	20–40–60	0.1–5–25–50	10–20–30	0–160 in steps of 20
0–45–90	20–40–60	0.1–5 – 25–50	10–20–30	0–160 in steps of 20
0–45–90	20–40–60	0.1–5–25–50	10–20–30	0–160 in steps of 20

From the above mentioned combinations, a total of 30,240 cases have been generated from the simulation model shown in Figure 1. For all faulty cases, the fault duration is set to 2 periods (0.04 s). Voltage and current signals are measured at the sending end.

3. Proposed fault classification technique

The proposed fault classification scheme is based on a combined ST-SVM and its block diagram is given in Figure 2. In the proposed technique, fault classification and identification of the faulty section are performed in 3 steps; preprocessing, feature extraction, and classification and decision. These steps are given in detailed as follows.

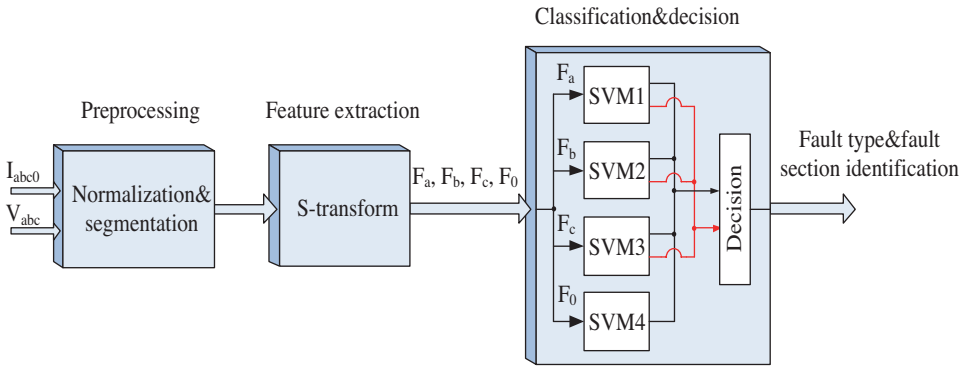

Figure 2. The proposed scheme for fault classification and faulty section identification.

3.1. Preprocessing

In this step, measured signals are subjected to normalization and segmentation processes. In normalization process, the signals are relatively scaled to have a maximum value of +1 and a minimum value of –1. For current and voltage signals, the samples are taken for 1 cycle ahead and 1 cycle back from the fault inception in the segmentation process. Thus, the size of the signals can significantly be reduced in the segmentation process.

3.2. Feature extraction by using S-transform

It is extremely important to select suitable features of signal(s) for fault classification and identification of faulty sections. Appropriate selection of features reduces the computational burden on the classifiers because extracted features by a signal processing technique are applied as input to the classifier. The ST is a time-frequency analysis method combining properties of the short-time Fourier transform and WT. It provides frequency-dependent resolution while maintaining a direct relationship with the Fourier spectrum. The ST of a signal $h(t)$ is defined as follows [30]:

$$STFT\,(\tau, f)\ = \int h(t)\,\omega(\tau - t)\,e^{-j2\pi ft}dt, \tag{1}$$

where the window function is a scalable Gaussian window given in Eq. (2):

$$\omega(t,\,\sigma) = \frac{1}{\sigma\sqrt{2\pi}}e^{-\frac{t^2}{2\sigma^2}} \tag{2}$$

and

$$\sigma = \frac{1}{|f|}. \tag{3}$$

Eq. (4) is obtained by combining Eq. (2) and Eq. (3).

$$S(\tau,\,f) = \int_{-\infty}^{+\infty} h\,(t)\frac{|f|}{\sqrt{2\pi}}e\,\frac{(\tau - t)^2 f^2}{2}\,e^{-j2\pi ft} \tag{4}$$

For a time sampling interval of T, a discrete time series of $h(t)$ is given in the form of $h[kT]$, $k = 0,\ 1,\ 2,\ ....,\ N-1$. Discrete Fourier transform of $h(t)$ is also presented as follows [31]:

$$H\,\left[\frac{n}{NT}\right] = \frac{1}{N}\sum_{k=0}^{N-1} h\,(kT)\;e^{\left(-\frac{j2\pi\,n\,k}{N}\right)}, \tag{5}$$

where n = 0, 1, ..., N – 1. Using Eq. (8), the ST of a discrete time series *h(kT)* is given by letting $\tau \to jT$ and $f \to n/NT$ as in Eq. (6):

$$S\,\left[jT, \frac{n}{NT}\right] = \sum_{m=0}^{N-1} H\,\left[\frac{m+n}{NT}\right]\,e^{-\frac{2\pi^2 m^2}{n^2}}\,e^{\frac{i2\pi\,m\,k}{N}}, n \neq 0. \tag{6}$$

For $n = 0$, it is equal to the constant defined in Eq. (7).

$$S\,[jT,\,0] = \frac{1}{N}\sum_{m=1}^{N-1} h\,\left(\frac{m}{NT}\right) \tag{7}$$

Here, $j,\ m\ =\ 0,\ 1, ...,\ N\ -\ 1$ and $n\ =\ 1, ..., N-1$. The discrete inverse of the ST is presented as:

$$h\ [jT] = \sum_{n=0}^{N-1} \left\{ \frac{1}{N} \sum_{k=0}^{N-1} S\ \left[jT,\ \frac{n}{NT}\right] \right\} e^{\frac{i2\pi\, n\, k}{N}} \tag{8}$$

The output of the ST is a matrix with $k \times n$ dimensions called the S-matrix. Each element of the ST-matrix has a complex value. The ST-amplitude (STA) matrix is obtained as [31]:

$$A(kT,\ f) = |S\ [kT,\ n/NT]\,|\,. \tag{9}$$

In this study, the 8 distinctive features are obtained from the ST for each signal. In Figure 2, F_a, F_b, and F_c represent the features extracted from 3-phase signals while F_0 represents features extracted from the ground current. A total of 56 distinctive features are extracted from the feature extractor (24 features for 3-line currents, 24 features for 3-line voltages, and 8 features for zero sequence current). In the ST, feature extraction is carried out by applying standard statistical techniques to the components of the STA matrix as well as directly on the STA matrix contours [21]. These features are useful for detection and classification of relevant parameters of the fault signals.

The feature extraction using ST consists of 3 steps. In step 1, the feature extraction process from the TMA-plot is performed. In the end of the process, features such as the maximum (F_1), minimum (F_2), standard deviation (F_3), and magnitude factor (F_4) are obtained from the TMA-plot. The magnitude factor of the TMA-plot can be calculated as follows [21]:

$$F_4 = \frac{1}{F_S}(1 + (F_1 + F_2 - (F_S)). \tag{10}$$

In Eq. (10), F_S is equal to $\mathrm{F}_1 + \mathrm{F}_2$ for a faultless signal. In addition, it is known that features except for F_1 and F_2 do not contribute to the magnitude factor of the TMA-plot. Step 2 includes feature extraction from the FMA-plot. Here, total harmonic distortion and mean square root of signals are obtained from the FMA-plot of the STA-matrix. These features are labeled as F_5 and F_6, respectively.

In step 3, a feature extraction process based on TF-contour is carried out and 2 distinctive features of signals are obtained from its STA-matrix. They are the standard deviation of contour having the largest frequency amplitude (F_7) and the energy of contour having the largest frequency amplitude of TF-contour (F_8). Segmented and normalized 3-phase currents and the FMA-plot, TMA-plot, and TF-contour of their STA-matrix for a 3-phase current in the case of *ag* fault at 220 km and in front of the series capacitor (SC) and system parameters including load angle 20°, compensation level 60%, fault inception angle 90°, and fault resistance 50 Ω are shown in Figures 3a, 3b, 3c, and 3d, respectively. From the FMA-plot, it is seen that frequency in peak value of current represents the fundamental frequency component of the signal. In the faulty phase, amplitude of the fundamental frequency component increases whereas amplitude of the fundamental frequency component in faultless phases remains approximately constant. From the TMA-plot, it is seen clearly that amplitude of the faulty signal has increased significantly once a fault has started. However, there is not a noticeable change in amplitude of the faultless phases. Furthermore, the starting instant of fault can be visually seen from TF-contours. This feature of TF-contours can be also used for fault detection.

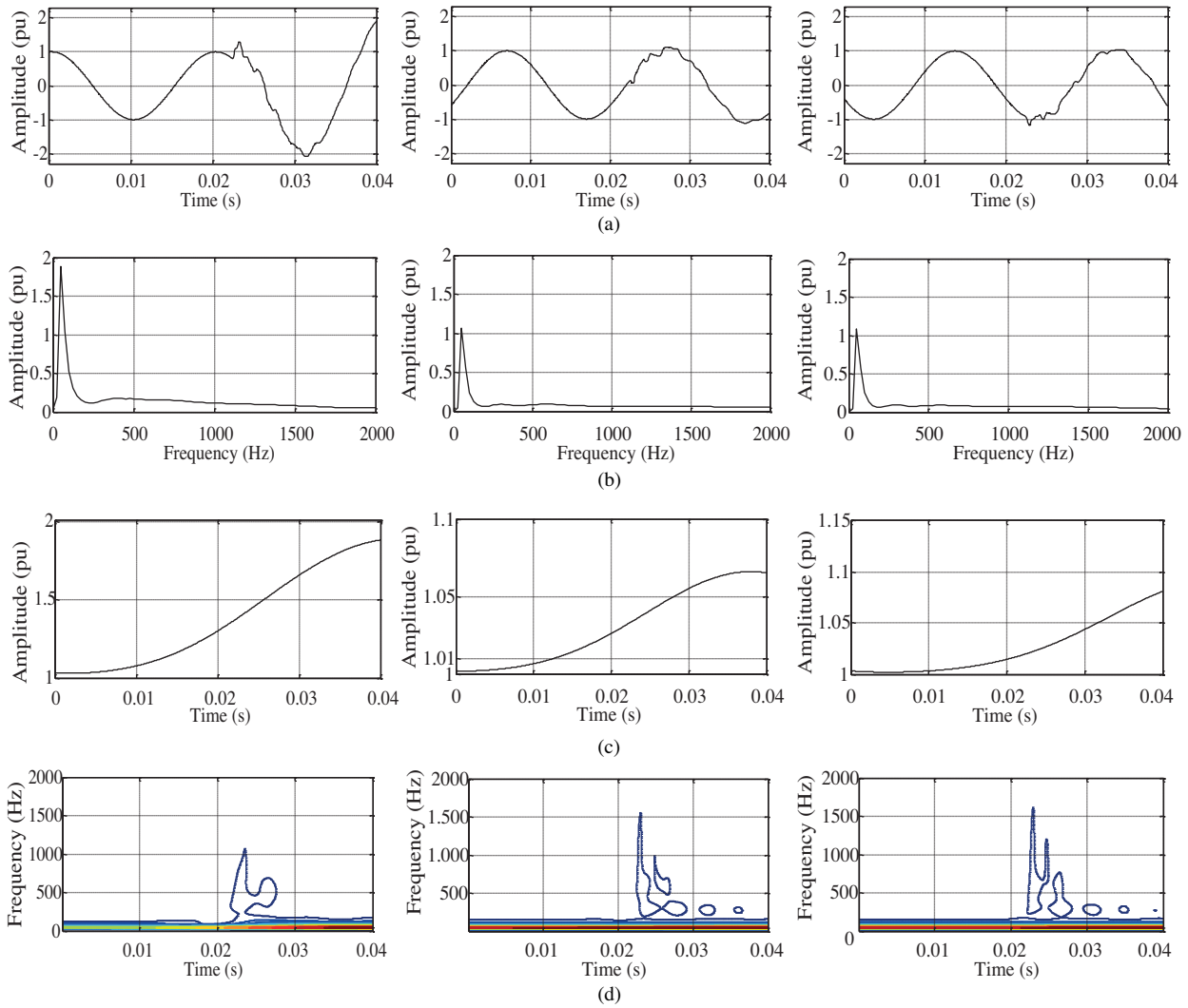

Figure 3. Outputs of STA-matrix for 3-phase current in the case of *ag* fault: a) segmented and normalized 3-phase current, b) FMA-plot for STA matrix of 3-phase current, c) TMA-plot for STA-matrix of 3-phase current, and d) TF-contour for STA matrix of 3-phase current.

The detection of ground fault from 3-line currents or voltages is difficult. Therefore, zero sequence current is used in order to identify easily the ground fault in this study. Figure 4a presents segmented and normalized zero sequence current, whereas Figures 4b–4d present time-frequency components (FMA-plot, TMA–plot, and TF-contour) derived from the STA-matrix of segmented and normalized zero sequence currents. It is clearly seen from Figure 4a that there is no value of zero sequence current in faultless conditions (up to 0.0225 s) but the current takes any value in the fault case. Figure 4b shows that the signal contains high-frequency components due to the fault condition. Change in the amplitude of zero sequence current can be obviously seen from Figure 4c after the fault case. As seen from Figure 4d, there are no frequency components before the fault is started. However, frequency components appear in this contour after the faulty case. These features facilitate detection of the ground faults.

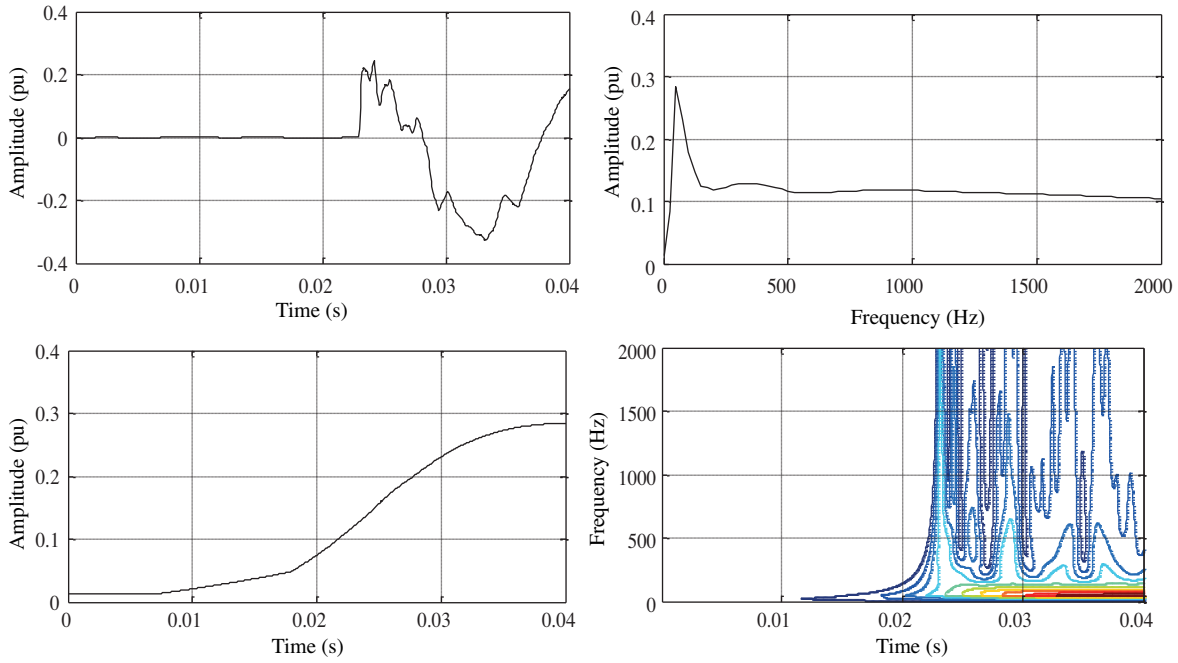

Figure 4. Component derived from STA-matrix of zero sequence current: a) segmented and normalized zero sequence currents, b) FMA-plot, c) TMA-plot, and d) TF-contour.

In Figure 5, variations of feature F_3 for LG faults including *ag*, *bg*, and *cg* are depicted for 300 randomly selected samples. Samples up to the 50th belong to the *fsc* set whereas the rest of the samples are in the *bsc* set. The value of feature F_3 for the faulty phase varies in the range of about 3×10^{-4} to 14×10^{-4} in the case of an *ag* fault as shown in Figure 5a. However, this value changes approximately between 0.5×10^{-4} and 3×10^{-4} in the case of the *ag* fault occurring after the SC. Figures 5b and 5c show that similar events take place for *bg* and *cg* faults both after and before the SC. Additionally, it is shown that feature F_3 takes different values in the faultless phase as well as different positions of the fault. Similarly, other features described above also have important contributions for fault-type classification and identification of faulty sections.

4. Fault classification and faulty section identification by SVMs

Recently, SVMs have been used as effective tools for fault classification in power systems [3,8,18,29,32]. This approach constructs the separating hyperplane for pattern recognition. A binary classification problem handles a set of examples $\{x_i, y_i\}$ with $1 \leq i \leq \ell$ (ℓ is the size of the example). Each example is part of a class labeled as y_i. The SVM classifier looks for an optimal hyperplane separating the opposite classes. The x points, which lie on this hyperplane, satisfy the equation $w.x + b = 0$. w is a normal vector of the separating hyperplane and b is a scalar called the bias term. The SVM searches for maximum separating hyperplane to satisfy Eq. (11). If Eq. (11) is satisfied, then examples are linearly separated [33].

$$s_i \ (w.x_i + \ b) \ \geq \ 1 \tag{11}$$

The optimal separating hyperplane is called the separating hyperplane achieving the maximum distance between the plane and the nearest data. Figure 6 shows an example for the optimal separating hyperplane with 2 datasets.

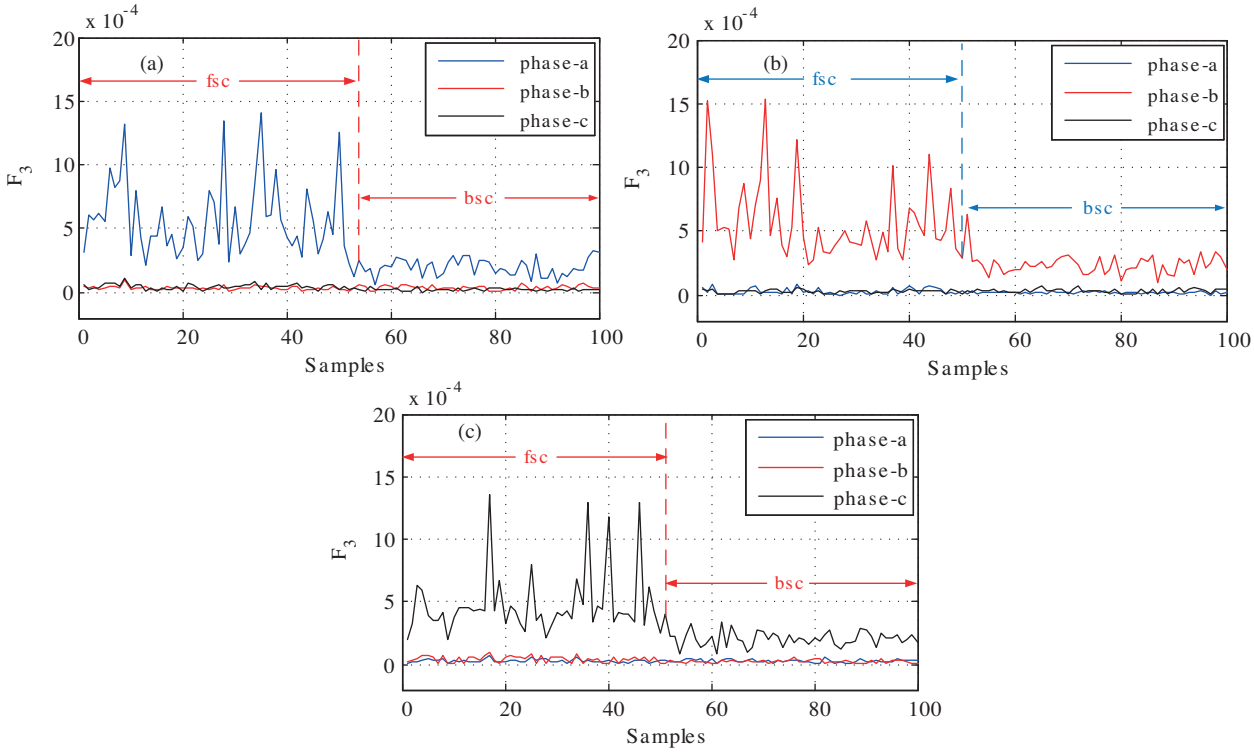

Figure 5. Variation of feature F_3 for LG faults: a) *ag* fault, b) *bg* fault, and c) *cg* fault.

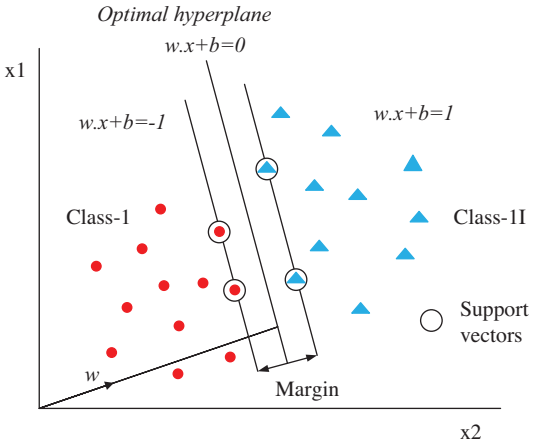

Figure 6. An example for the optimal separating hyperplane with 2 datasets.

The geometrical margin is founded as $\|w\|^{-2}$ from this figure. The solution of following quadratic optimization problem gives optimal hyper-plane [34]:

$$\begin{aligned} &\underset{w}{\text{Minimize}} \quad \tfrac{1}{2}\|w\|^2 \\ &\text{Subject to} \quad s_i\ (x_i \,.\, w\ +\ b)\ \geq\ 1 \end{aligned} \qquad . \tag{12}$$

This problem can be solved by a Lagrangian multiplier as follows:

$$\frac{1}{2}\ \|w\|^2 - \sum_{i=1}^{\ell} c_i\ (s_i\ (\ w\,.\,x_i + b)\ -\ 1). \tag{13}$$

The Lagrangian has to be minimized with respect to the primal variables w and b while it has to be maximized with respect to the dual variable c_i. The Karush–Kuhn–Tucker (KKT) conditions lead to finding the solution vector in terms of the training pattern, $w\ = \sum_{i=1}^{\ell}\ c_i\, s_i\, x_i$ for some $c_i\ \geq\ 0$. The solution in its dual form is used to solve this problem [34]:

$$\begin{aligned} &\max\ \ -\tfrac{1}{2}\sum_{i,\,j=1}^{\ell} c_i\, c_j\, s_i\, s_j\, \Phi\,(x_i)\,\Phi(x_j)\ +\ \sum_{i=1}^{\ell} c_i = -\tfrac{1}{2}\sum_{i,\,j=1}^{\ell} c_i\, c_j\, s_i\, s_j\, K(x_i, x_j)\ +\ \sum_{i=1}^{\ell} c_i \\ &\text{Subject to}\ \sum_{i=1}^{\ell} c_i\, s_i =\ 0, \qquad c_i \geq\ 0 \end{aligned} \tag{14}$$

where $K\,(x_i,\,x_j)$ is kernel function that is a nonlinear function and can be defined as follows:

$$K\,(x_i, x_j) = \Phi\,(x_i)\ \Phi(x_j). \tag{15}$$

A SVM then uses the convolution of the scalar product to build, in input space, the following nonlinear decision function:

$$f(x) = sign\ \left(\sum_{i=1}^{\ell} c_i\, s_i K\,(x,\,x_i)\ +\ b\right). \tag{16}$$

A separating hyperplane does not exist if training data are not linearly separable. The learning task in Eq. (17) is essentially the same as that indicated in Eq. (12) if regularization parameter C and slack variable ξ_i are assumed to be zero. The classifier attempts to separate the data by minimizing the objective function [34].

$$\begin{aligned} &\min_{w} \qquad \tfrac{1}{2}\ \|w\|^2 + C\sum_{i=1}^{\ell}\xi_i \\ &\text{Subject to} \quad s_i\,(x_i\,.\,w\ +\ b)\ \geq\ 1-\xi_i, \quad \xi_i \geq\ 0\ for\ all\ i \end{aligned} \tag{17}$$

In this study, the Gaussian kernel function, which is one of the most commonly used kernels, is preferred. It is defined as follows:

$$K\,(x_i,\,x_j) = \exp\ \left(\frac{-\,|x-x_i|^2}{2\sigma^2}\right), \tag{18}$$

where σ is the width parameter of the Gaussian function. The classification performance of the SVM depends on parameters C and σ.

Basically, multiclass SVM classifiers can be formed by 2 types of approaches. The first approach aims to modify the design of the SVMs to incorporate the multiclass learning in the quadratic solving algorithm and the other approach combines several binary classifiers [35]. In the second approach, methods such as *one-against-rest* and *one-against-one* have been proposed. In this paper, the *one-against-one* method is used for multiclass classification. The feature vectors obtained from the ST are used as an input to the SVMs of the respective

phases (SVM1, SVM2, and SVM3) and the SVM of the ground (SVM4). As previously said, detection of the ground fault cannot be possible only from the fundamental components of voltages and currents. Therefore, zero sequence current is used to detect the ground faults. The SVMs of particular phases (SVM1, SVM2, and SVM3) have 2 outputs designating the faulted phase (output 1) and faulty section (output 2). SVM4 has one output indicating ground fault. For accurate fault classification, training of SVMs should be fulfilled by a group of training data. For this purpose, 300 faulty cases randomly chosen for each fault type have been considered as the training set for SVM classifiers. After the training of the SVMs, classification performance of the proposed technique was tested with the remaining dataset.

4.1. Parameter selection and training of SVM

As stated previously, training and testing data are generated for 10 types of faults with varying fault locations, fault resistance, compensation level, and fault inception angle. The input patterns to SVMs classifiers consist of distinctive features of phase voltages (V_{abc}), phase currents (I_{abc}), and ground current (I_0). To obtain a good classification performance from the SVM classifier, its parameters such as regularization parameter C and kernel parameters such as σ for radial basis function (RBF) have to be carefully chosen. In the literature, several studies have been done to evaluate classification performance of kernel functions in different areas. The studies show that satisfactory classification performance is obtained by using the RBF kernel because it indicates properties of both sigmoid and linear kernel functions depending on the selected parameter range [36,37]. In this paper, the Gaussian RBF is used and the optimum values of its parameters are found by a search process. This process includes a wide range of variation of 2 parameters: C and σ. These ranges are considered for $C = 1$–2^{16} by step $2^{0.5}$ and $\sigma = 2^{-4}$ to 2^{6} by step $2^{0.5}$. The parameters of SVMs giving the highest accuracy are considered as optimal parameters. The optimum values of C and σ are found as 11,585 and 32, respectively. Similarly, the values of these parameters for other SVMs are given in Table 3. In addition, once the SVMs are learned with these parameters, all parameters of the trained SVMs are fixed and then used in retrieval mode for testing the capabilities of the system.

Table 3. Optimum values for the parameters of SVMs obtained by search process.

Classifiers	Parameters	
	C	σ
SVM1	11,585	32
SVM2	8192	64
SVM3	16,384	22.627
SVM4	2896.3	0.1768

5. Results and discussion

To evaluate the validity of the proposed technique, the simulation model has been run for different combination of system parameters. A total of 30,240 cases have been obtained from this model. The training dataset is composed of 3000 cases selected randomly with 300 cases from each event. Testing of the classifier is performed by using the remaining 27,240 data.

After training of the SVM classifier, overall accuracy for fault classification of the proposed method for different types of faults including LG, LL, LLG, and LLL-LLLG with various operating conditions is presented in Table 4. It can be seen that the proposed method classifies 26,911 out of 27,240 test data correctly and

overall accuracy is obtained as 98.754%. The highest classification rate is 99.449% for LG faults, whereas the lowest classification accuracy is found as 97.687% for LL faults.

Table 4. Performance of the proposed technique for fault classification.

Fault type	Test	Training	True	False	Overall accuracy (%)
LG	8172	900	8127	45	99.449
LLG	8172	900	8116	56	99.314
LLL-LLLG	2724	300	2685	39	98.568
LL	8172	900	7983	189	97.687
Total	27,240	3000	26,911	329	98.754

The performance of the proposed method is also investigated by making comparisons with the ST-NN method, which is widely used in many practical applications. In ST-NN, distinctive features of 3-phase signals and zero sequence current are extracted by the ST (a total of 54 distinctive features). Extracted features are then given as input to NN classifiers. Fault classification performance of the proposed method is depicted in Table 5 as compared with ST-NN. It has been found that overall accuracy of ST-NN is 96.389%, which is lower than that obtained by the proposed method.

Table 5. Classification performance of ST-NN and the proposed method for fault classification.

Fault type	This study (%)	ST-NN (%)
LG	99.449	96.243
LLG	99.314	97.479
LLL-LLLG	98.568	95.631
LL	97.687	96.206
Total	98.754	96.389

A comparison among previous studies and the proposed ST-SVM is depicted in Table 6 for different types of fault. The obtained results show that the proposed method has better classification performance compared with previous studies. The highest accuracy among previous studies is obtained as 98.703% by [3], while the overall accuracy of the proposed method is 98.754%.

Table 6. Performance comparison among the proposed method and previous studies for fault classification.

Fault type	[3]	[8]	[17]	[26]	This study
LG	97.447	96.230	90.729	98.56	99.449
LLG	98.611	97.050	97.754	97.26	99.314
LLL-LLLG	100	94.325	91.458	97.62	98.568
LL	99.616	88.333	91.631	96.84	97.687
Overall accuracy (%)	98.703	93.917	92.893	97.57	98.754

Performance of the proposed method for identification of faulty sections is also presented in Table 7 as compared with ST-NN and [26]. This table reveals that the proposed method shows a more effective section identification performance than results of both ST-NN and [26].

Table 7. Performance comparison among the proposed method, ST-NN, and a previous study for identification of faulty section.

Fault type	This study (%)	ST-NN (%)	[26]
LG	99.862	95.853	99.65
LLG	99.069	94.806	98.56
LLL-LLLG	98.751	96.585	98.62
LL	98.188	95.324	97.62
Overall accuracy (%)	98.967	95.642	98.613

6. Conclusion

In this paper, a combined relaying scheme based on ST-SVM for protection of the SCTLs is proposed. The proposed method uses 3-line voltage and current signals and zero sequence current to classify different types of faults and identify faulty sections. In the proposed method, which is performed in 3 stages, the ST feature extractor is responsible for extracting the distinctive features of signals. The distinctive features of signals are used as input to SVM classifiers. The outputs of SVMs then classify the type of fault and identify the faulty section. The feasibility of the developed technique has been tested on an extensive dataset of 27,240 test cases including a wide range of operating conditions. It is obviously seen from simulation results that the proposed method manages to classify and identify the faults at high accuracy in spite of the presence of the series capacitor and MOV. In addition, the faults involving the ground are easily detected by usage of zero sequence current. The classification and section identification accuracies of the proposed technique have been found to be 98.754% and 98.967%, respectively. The robustness of the proposed method for changing of parameters such as compensation level, fault inception angle, load angle, different location of fault, and source impedance is also seen from the results. It can be concluded from the results that the proposed method based on ST-SVM can provide a reliable relaying scheme in SCTLs.

References

[1] J. Woodworth, "MOV protection of series capacitor banks", Arrester Factors008, 2008. Available at http://arresterworks.com/ArresterFacts_files/ArresterFacts%20008%20-%20MOV%20Protection%20of%20Series%20Capacitor%20Banks.pdf.

[2] A.K. Pradhan, A. Routray, S. Pati, D.K. Pradhan, "Wavelet-fuzzy combined approach for fault classification of a series-compensated transmission line", IEEE Transactions on Power Delivery, Vol. 19, pp. 1612–1618, 2005.

[3] U.B. Parikh, B. Das, R. Maheshwari, "Fault classification technique for series compensated transmission line using support vector machine", International Journal of Electrical Power and Energy Systems, Vol. 32, pp. 629–636, 2010.

[4] O. Özgönenel, G. Önbilgin, Ç. Kocaman, "Transformer protection using the wavelet transform", Turkish Journal of Electrical Engineering & Computer Sciences, Vol. 13, pp. 119–135, 2005.

[5] E. Kılıç, O. Özgönenel, Ö. Usta, D. Thomas, "PCA based protection algorithm for transformer internal faults", Turkish Journal of Electrical Engineering & Computer Sciences, Vol. 17, pp. 125–142, 2009.

[6] M.A. Khan, O. Ozgonenel, M.A. Rahman, "Wavelet transform based protection of stator faults in synchronous generators", Electric Power Components and Systems, Vol. 35, pp. 625–637, 2007.

[7] O. Ozgonenel, E. Kilic, M.A. Khan, M.A. Rahman, "A new method for fault detection and identification of incipient faults in power transformers", Electric Power Components and Systems, Vol. 36, pp. 1226–1244, 2008.

[8] U.B. Parikh, B. Das, R.P. Maheshwari, "Combined wavelet-SVM technique for fault zone detection in a series compensated transmission line", Transactions on Power Delivery, Vol. 23, pp. 1789–1794, 2008.

[9] A.K. Pradhan, A. Routray, B. Biswal, "Higher order statistics-fuzzy integrated scheme for fault classi?cation of a series compensated line", Transactions on Power Delivery, Vol. 19, pp. 891–893, 2004.

[10] Q.Y. Xaun, Y.H. Song, A.T. Johns, R. Morgan, D. Williams, "Performance of an adaptive protection scheme for series compensated EHV transmission systems using neural networks", Electric Power System Research, Vol. 36, pp. 57–66, 1996.

[11] D. Novosel, B. Bachman, D. Hart, Y. Hu, M.M. Saha, "Algorithms for locating faults on series compensated lines using neural network and deterministic methods", Transactions on Power Delivery, Vol. 11, pp. 1728–1736, 1996.

[12] Y.H. Song, A.T. Johns, Q.Y. Xuan, "Artificial neural network based protection scheme for controllable series compensated EHV transmission lines", IEE Proceedings: Generation, Transmission, and Distribution, Vol. 143, pp. 535–540, 1996.

[13] Y.H. Song, Q.Y. Xuan, "Protection scheme for EHV transmission systems with thyristor controlled series compensation using radial basis function neural networks", Electric Machines and Power Systems, Vol. 25, pp. 553–565, 1997.

[14] P.K. Dash, A.K. Pradhan, G. Panda, "Application of minimal radial basis function neural network to distance protection", Transactions on Power Delivery, Vol. 16, pp. 68–74, 2001.

[15] A.Y. Abdelaziz, A.M. Ibrahim, M.M. Mansour, H.E. Talaat, "Modern approaches for protection of series compensated transmission lines", Electric Power Systems Research, Vol. 75, pp. 85–98, 2005.

[16] G. Feng, G.B. Huang, Q. Lin, R. Gay, "Error minimized extreme learning machine with growth of hidden nodes and incremental learning", Transactions on Neural Networks, Vol. 20, pp. 1352–1357, 2009.

[17] U.B. Parikh, B.R. Bhalja, R.P. Maheshwari, B. Das, "Decision tree based fault classification scheme for protection of series compensated transmission lines", International Journal of Emerging Electric Power Systems, Vol. 8, pp. 1–12, 2007.

[18] P.K. Dash, S.R. Samantaray, G. Panda, "Fault classi?cation and section identification of an advanced series-compensated transmission line using support vector machine", Transactions on Power Delivery, Vol. 22, pp. 67–73, 2007.

[19] V. Malathi, N.S. Marimuthu, S. Baskar, "A comprehensive evaluation of multicategory classification methods for fault classification in series compensated transmission line", Neural Computing and Applications, Vol. 19, pp. 595–600, 2009.

[20] A.I. Megahed, A.M. Moussa, A.E. Bayoumy, "Usage of wavelet transform in the protection of series-compensated transmission lines", Transactions on Power Delivery, Vol. 21, pp. 1213–1221, 2006.

[21] M. Uyar, S. Yildirim, M.T. Gencoglu, "An expert system based on S-transform and neural network for automatic classification of power quality disturbances", Expert Systems with Applications, Vol. 36, pp. 5962–5975, 2009.

[22] M.J. Dehghani, "Comparison of S-transform and wavelet transform in power quality analysis", World Academy of Science, Engineering and Technology, Vol. 50, pp. 395–398, 2009.

[23] R.G. Stockwell, L. Mansinha, R.P. Lowe, "Localization of the complex spectrum: the S-transform", Transactions on Signal Processing, Vol. 44, pp. 998–1001, 1996.

[24] M.V. Chilukuri, P.K. Dash, "Multiresolution S-transform-based fuzzy recognition system for power quality events", Transactions on Power Delivery, Vol. 19, pp. 323–330, 2004.

[25] M. Uyar, S. Yıldırım, M. T. Gençoğlu, "Güç kalitesindeki bozulma türlerinin sınıflandırılması için bir örüntü tanıma yaklaşımı", Gazi Üniversitesi Müh. Mim. Fak. Dergisi, Vol. 26, pp. 41–56, 2011 (article in Turkish).

[26] S.R. Samantaray, P.K. Dash, "Pattern recognition based digital relaying for advanced series compensated line", International Journal of Electrical Power and Energy System, Vol. 30, pp. 102–112, 2008.

[27] Z. Moravej, M. Pazoki, A.A. Abdoos, "A new approach for fault classification and section detection in compensated transmission line with TCSC", European Transactions on Electrical Power, Vol. 21, pp. 997–1014, 2011.

[28] H. Shu, X. Tian, P. Cao, C. Liu, "Fault classification and location of power transmission lines with S-transform and artificial neural network", International Conference on Energy Systems and Electrical Power, Energy Procedia, Vol. 13, pp. 5991–5998, 2011.

[29] H. Erişti, Y. Demir, "A new algorithm for automatic classification of power quality events based on wavelet transform and SVM", Expert Systems with Applications, Vol. 37, pp. 4094–4102, 2010.

[30] S.S. Sahu, G. Panda, N.V. George, "An improved S-transform for time-frequency analysis", International Advance Computing Conference, pp. 315–319, 2009.

[31] Y.H. Wang, "The tutorial: S-transform lecture note", Graduate Institute of Communication Engineering, National Taiwan University.

[32] S. Ekici, "Classification of power system disturbances using support vector machines", Expert Systems with Applications, Vol. 36, pp. 9859–9868, 2009.

[33] B. Ravikumar, D. Thukaram, H.P. Khincha, "Comparison of multiclass SVM classification methods to use in a supportive system for distance relay coordination", Transactions on Power Delivery, Vol. 25, pp. 1296–1305, 2010.

[34] V.N. Vapnik, Statistical Learning Theory, New York, Wiley, 1998.

[35] J. Weston, J.C. Watkins, "Multi-class support vector machines", Technical Report, Department of Computer Science, University of London, 1998.

[36] S.S. Keerthi, C.J. Lin, "Asymptotic behaviors of support vector machines with Gaussian kernel", Neural Computation, Vol. 15, pp. 667–1689, 2003.

[37] B. Schölkopf, K.K. Sung, C.J. Burges, F. Girosi, P. Niyogi, T. Poggio, V. Vapnik, "Comparing support vector machines with Gaussian kernels to radial basis function classifiers", Transactions on Signal Processing, Vol. 45, pp. 2758–2765, 1997.